

A Novel Methodology for Incipient Ball Screw Backlash Measurement Using Capacitive Sensor

Marcella Miller¹, Xu Han¹, Gregory William Vogl², Anita Penkova³, and Xiaodong Jia¹

Abstract—Creating a reliable indicator to describe the degradation of ball screws remains a challenging task. Current vibration-based prognostic methods are vulnerable to unknown noise or system disturbances. To address this challenge, our study offers a new method to monitor the developing trend of incipient backlash in a ball screw assembly using a capacitive sensor. The suggested method for measuring backlash is noncontact and in situ, providing direct evidence of ball screw degradation. Furthermore, a rigorous backlash measurement model, referred to as the path error model, is brought forward. This model serves as the foundation for a proposed procedure for backlash measurement. The method is validated in a run-to-failure (RTF) experiment, and the results indicate a promising upward trend in the backlash that agrees with the vibrational signatures.

Index Terms—Ball screw, linear motion control, predictive maintenance, smart manufacturing.

I. INTRODUCTION

THE prognosis of ball screw degradation (or precision loss) is a critical research topic across many industrial applications that have stringent precision requirements, such as high-precision computer numerical control (CNC) machining and wafer-handling robots [1], [2], [3]. At an early stage, the ball screw degradation is characterized by a gradual loss of rigidity at the ball nut connection [4], [5]. Over time, this rigidity loss develops into backlash, which refers to a small clearance between the rollers and the raceway. As the backlash continues to develop, it increasingly compromises operational precision and ultimately necessitates the replacement of a degraded component with a new one. In the context of CNC machine tools, the acceptable backlash typically ranges from 5 to 17 μm [6].

Practical measurements of backlash error can be accomplished using dial indicators [7] or optical gratings [8].

Received 30 May 2024; revised 17 December 2024; accepted 13 January 2025. Date of publication 25 February 2025; date of current version 10 March 2025. This work was supported in part by U.S. Department of Commerce, National Institute of Standards and Technology under Award 60NANB21D114. The Associate Editor coordinating the review process was Dr. Shisong Li. (Corresponding author: Marcella Miller.)

Marcella Miller, Xu Han, and Xiaodong Jia are with the Department of Mechanical and Materials Engineering, College of Engineering and Applied Science, University of Cincinnati, Cincinnati, OH 45221 USA (e-mail: mille5mc@mail.uc.edu; hanx7@mail.uc.edu; jiaxg@ucmail.uc.edu).

Gregory William Vogl is with the Engineering Laboratory, National Institute of Standards and Technology, Gaithersburg, MD 20899 USA (e-mail: gregory.vogl@nist.gov).

Anita Penkova is with the Department of Aerospace and Mechanical Engineering, Viterbi School of Engineering, University of Southern California, Los Angeles, CA 90089 USA (e-mail: penkova@usc.edu).

Digital Object Identifier 10.1109/TIM.2025.3545168

However, both the methods are limited to detecting relatively significant backlash (typically exceeding 2 μm), which is important for error compensation or control. The exploration of the developing trend of incipient backlash ($\leq 2 \mu\text{m}$) for prognosis purposes is still limited, despite its potential to offer direct evidence of system degradation.

From the perspective of degradation prognosis or predicting remaining useful life, monitoring incipient backlash may offer several advantages over existing methods such as preload loss estimation [9], [10], [11] or vibration analysis [12]. The simulative study on preload loss in [13] suggests a two-stage pattern. The first stage involves a rapid decrease in preload at the onset of the lifecycle (roughly the first 100 operation hours). The second stage is characterized by a gradual reduction in the preload. Under some circumstances, the trend of preload reduction in the latter stage could be nearly flat and thus unsuitable for health prognosis. In addition, vibration-based health prognosis is susceptible to unknown sources of noise or distances. In previous run-to-failure (RTF) experiments [12], it was found that the oil debris could cause unexplainable system vibration and thus impact the prognosis results significantly. Therefore, this article aims to propose a new method to monitor the developing trend of incipient backlash in a ball screw assembly, providing direct evidence for system degradation.

The core innovation lies in the development of a novel measurement method for detecting incipient backlash below 2 μm , while effectively mitigating the substantial positional shifts induced by thermal expansions (approximately 15–20 μm). The proposed backlash measurement method is noncontact and in situ, and it offers submicrometer measurement precision. The measured incipient backlash in the designed RTF experiment indicates a clear upward trend that matches very well with the vibrational signatures.

A. Literature Review

Backlash in ball screws refers to the axial clearance between the rollers and the raceway that develops over time due to system wear [4], [5]. When the ball screw reverses its direction of linear motion, this clearance results in a brief period of disengagement before the rollers re-engage in the opposite direction. This momentary disengagement leads to a minor amount of loss of movement, known as backlash error [14]. Backlash is a significant source of machining error and must be compensated for in high-precision machining

operations [3], [4]. The magnitude of the backlash error is often used to define the end-of-life of the ball screw, depending on the intended precision requirements.

Displacement sensors, such as laser interferometers and capacitive sensors, offer exceptionally precise position measurements at submicrometer or even subnanometer scales [15]. However, determining backlash in ball screws entails more than mere positional measurement, as backlash is discernible only during reversal motions. It is necessary to develop a comprehensive measurement framework to shape the assessment procedure to ensure the resulting value offers a direct measurement of backlash. The study in [8] used an optical grating to measure the reversal error among three target points $A \rightarrow B \rightarrow C$, where $B \rightarrow C$ is the reversal motion back to the original position A. The detailed derivation of this three-point model is elaborated on in the Appendix (model A1). Based on the three-point model in [8], this article proposes to consider the bounce error of each motion path, yielding a better understanding of backlash modeling.

Other studies have used laser interferometers for backlash measurements to verify simulation results under laboratory conditions [16], [17]. However, the setup of a laser interferometer system, which includes the laser head, beam splitter, photograph decoder, etc., is often too complex for practical use [18]. Moreover, the thermal error, which normally contributes 40%–70% of the total positioning error in a machine tool [19], [20], is not considered in these studies. Therefore, the development of a methodology for noncontact, real-time, submicrometer precision, and direct measurement of backlash remains an open area of research. A capacitive sensor was chosen for this application for its high precision and ease of setup. It is worth noting that capacitive sensors have been used in machine tools to measure position errors, thermal errors, or geometric errors [21], [22], [23]. However, to the best of the authors' knowledge, this is the first attempt to use capacitive sensors for measuring incipient backlash.

The existing methods for ball screw prognosis primarily focus on vibration analysis. Various degradation indicators are proposed and obtained through the analysis of vibrations to estimate preload loss [24]. For example, the vibrational components around the ball pass frequency (BPF) under steady-state operation (i.e., constant operation speed and loading) are frequently used as an indicator to describe the preload loss [9]. A fixed-cycle feature test is implemented in [12] to assess vibrational characteristics under comparable operating conditions. Another approach involves tracking the shift of the axial natural frequency (ANF) using the transient state vibration [10], [11]. This method simplifies the complex relationship between the ANF and the preload into a straightforward empirical equation, indicating that the ANF decreases as the preload reduces. In addition to these methods, an inertial sensor is also used as an indirect measurement of backlash by capturing positional shifts between positive and negative motions [25], [26].

However, using vibration analysis for health prognostics or the prediction of the remaining useful life presents challenges. Theoretical analysis suggests a two-stage degradation pattern for preload loss [13]. The first stage involves a rapid decrease

in preload at the onset of the lifecycle. The second stage is characterized by a gradual reduction in the preload [27]. The simulation results indicate that the trend of preload reduction could be nearly flat in the second stage. In addition, it is difficult to define a failure threshold without measuring the backlash. The relationship between preload reduction and incipient backlash development remains unknown.

B. Problem Statement

A review of the existing literature reveals that preload loss effectively describes the initial stage of ball screw degradation; however, identifying a reliable indicator to continuously describe further ball screw degradation, from incipient backlash development to a failure state characterized by large backlash, remains a challenge. Such an indicator is crucial for health prognosis. For example, in the case of a precision CNC machining operation, parts may be machined out-of-tolerance before the unmonitored developing backlash is noted. This can lead to excessive waste of scrapped parts or expensive rework. Wafer-handling robots that lose positioning accuracy due to backlash errors may crash, causing damage to the wafers and other highly sensitive equipment and disrupting upstream and downstream processes. Instead, by monitoring the developing backlash trend, operators and management can take action to correct the backlash and replace the degraded ball screw before a failure incurs extensive time and resource costs.

Therefore, this article presents a new method to measure the incipient ball screw backlash using a capacitive sensor. The measured backlash is expected to have submicrometer precision, and it can be used as direct evidence for early-stage ball screw degradation. The major novelties of the work are summarized as follows: 1) rigorous backlash measurement models are derived. The expectation and variance of the proposed measurement model are justified theoretically; 2) based on the theoretical analysis, a measurement routine is subsequently established. Novel strategies are developed to overcome the large position error induced by the thermal state of the ball screw; and 3) an RTF experiment is performed to verify that the measured incipient backlash can serve as a reliable indicator for early-stage ball screw degradation.

II. METHODOLOGY AND DESIGN OF EXPERIMENTS

A. Testbed Design for Backlash Measurement

Fig. 1 shows the experimental linear axis testbed used for this investigation. The linear axis was fixed on a concrete slab weighing approximately 1700 kg (3800 lbs.). The ball screw motor rotates to move the carriage along the X-axis. Two guideways, one on either side of the ball screw, contact four trucks with bearing balls to constrain the carriage to undergo nominally linear motion. The total useful length of the screw is just over 450 mm, and the pitch is 10 mm. To degrade the system, the carriage runs continuously, and the carriage is loaded with 100 kg (220 lbs.) of steel weights to accelerate the degradation process.

A Micro-Epsilon capaNCDT CS05 capacitive sensor (Fig. 1 inset) with a nominal sensitivity of $50 \mu\text{m}/\text{V}$ and a range of 0.5 mm is fixed at the motor side of the system to measure the

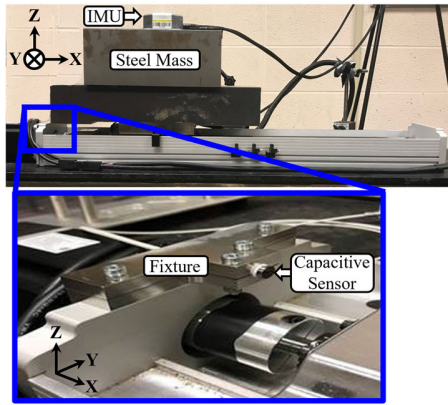


Fig. 1. Ball screw test bed used for experiments.

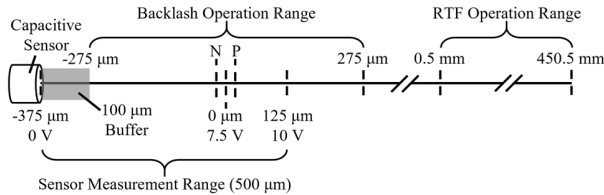


Fig. 2. Linear positions for the test bed setup.

position of the steel weights. The capacitive sensor measurement system also includes a Micro-Epsilon DT6110 oscillator, demodulator, and preamplifier signal conditioning box. Two triaxial accelerometers with a nominal sensitivity of 100 mV/g are epoxied to the ball nut, and an inertial measurement unit (IMU) identical to the one used in [25] is attached on top of the steel weights. Data from these sensors, as well as the speed and torque data from the controller, are collected throughout axis degradation.

To keep a consistent home position, the zero position is reset at a capacitive sensor reading of 7.5 V (375 μm from the face of the sensor) when the system is in a cold state. For all the motions, a 100- μm buffer is maintained between the sensor and the carriage load. During measurements, the operation range of the carriage may exceed the sensor measurement range, as shown in Fig. 2, but the significant axis positions at N, 0 μm , and P (described in more detail in Section II-B) are within the measurable range. Fig. 2 shows the relevant carriage positions for the linear axis experiments.

B. Proposed Method for Backlash Measurement

The backlash studied in this work can be considered a “reversal error.” As a linear positioning system degrades and preload is lost, gaps form between the bearing balls and the grooves of the ball screw. Since the reversal error can only be observed after a change in direction, two position measurements are required to produce one backlash calculation. A comparison of the measurements from before and after the reversal gives insight into the error accumulated from the reversal of motion.

Two methods for backlash measurement are proposed. Method A is called a “five-point model with bounce error,” and it is an improvement over the measurement model proposed in [8]. Method B is named a “path error model with bounce error.” Instead of calculating the difference between

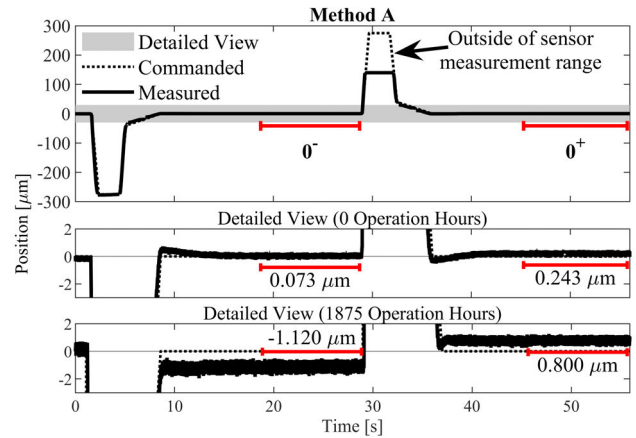


Fig. 3. General measurement procedure for method A with measurement examples from the RTF at 0 operation hours and at 1875 operation hours.

two measurement points, this model considers the path error caused by backlash, and an unbiased estimate of backlash can be obtained. Another difference between these two methods is the number of steps involved. In method A, the direction reversal occurs between measurement steps, while the direction reversal and measurement steps are simultaneous in method B. The reversal steps in method A do not need to remain within the measurement range of the capacitive sensor (see dashed line in Fig. 3) because they are not part of the testing, which may be useful in maintaining randomness in the measurements. However, there is a greater opportunity for unwanted error accumulation to occur since method A has additional steps.

1) *Method A: Five-Point Model (Model A3 in the Appendix):* For method A, the capacitive sensor takes measurements around the home position of 0 μm . One measurement, labeled 0^- , is obtained by approaching zero from the negative direction, and the other, labeled 0^+ , by approaching from the positive direction. Each measurement is obtained by averaging 10 s of stationary capacitive sensor data. Fig. 3 shows a comprehensive procedure for a single measurement using method A, including the detailed view of the actual capacitive sensor readings for a new ball screw at zero operation hours and a degraded ball screw at 1875 operation hours. When only the initial level of backlash error exists in the system, as shown in the detailed view of Fig. 3 for zero operation hours, the measured positions 0^- and 0^+ closely align with the commanded motion profile, exhibiting minimal error at 0.073 and 0.234 μm , respectively. In systems experiencing the onset of backlash, as depicted in the detailed view of Fig. 3 for 1875 operation hours, there is a deviation in the measured positions from the commanded positions, recorded at -1.120 and 0.800 μm .

The backlash for method A, M_A , can be calculated by (1). Method A is model A3 in the Appendix, where the detailed derivation can be found. Note that $E[M_A]$ is the expected value, $V[M_A]$ is the variance, and b is the backlash

$$\begin{aligned} M_A &= 0^+ - 0^- = b \\ E[M_A] &= b, \quad V[M_A] = 0. \end{aligned} \quad (1)$$

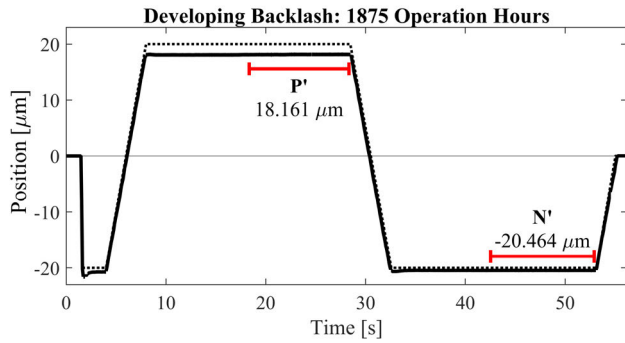


Fig. 4. General measurement procedure for method B with one measurement example from the RTF at 1875 operation hours.

This method can be implemented repeatedly to obtain multiple consecutive measurements. To acquire an accurate backlash reading for any given system state, 20 individual measurements (five sets of four) are collected and averaged. Before each set, a large, randomizing step is performed: the system moves to 20 mm and then returns to the home position. Although the expectation of the measurement is equal to the backlash, the variance of the model is zero, which is too ideal.

2) *Method B: Path Error Model (Model B2 in the Appendix):* Method B uses two different positions, P and N, for measurements that are symmetrically distributed around the home position. One measurement, denoted P', is taken at the positive position, and the other, denoted N', at the negative position. Fig. 4 shows the procedure for a single measurement using method B for a degraded ball screw at 1875 operation hours.

Unlike method A, which calculates the difference between points around the home position, method B calculates the path error, which offers an unbiased estimator of the backlash. In Fig. 4, the difference between P and N is considered the commanded path, while the actual path is between P' and N'. The measured motion loss caused by the backlash for method B (M_B) can be calculated by (2). Detailed derivations can be found in the Appendix for model B2

$$M_B = (P - N) - (P' - N') = b - e_B + e_C$$

$$E[M_B] = b, \quad V[M_B] = b^2/6. \quad (2)$$

This method can be implemented repeatedly to obtain multiple consecutive measurements. The expected value of the measurements is an unbiased estimator for the backlash with variance $b^2/6$. For method B, one large, randomizing step is performed before 15 measurements are collected and averaged for each system state.

C. Mitigating Thermal Effects

Thermal expansion has a significant effect on the measured positions in the system. As the ball screw operates at higher speeds (i.e., on the order of mm/s), thermal expansion occurs, which affects the measured positions. The thermal-expansion-induced positional shift observed in this experiment exceeds $15 \mu\text{m}$, whereas the targeted incipient backlash measurement is less than $2 \mu\text{m}$. Therefore, it is important to measure the backlash under the same thermal state to obtain consistent measurements of the incipient backlash.

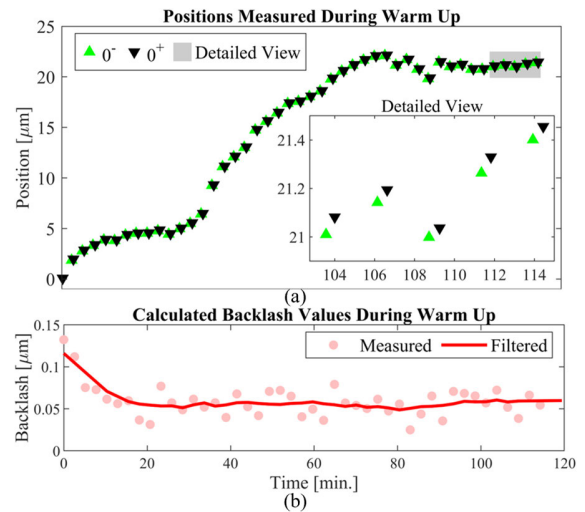


Fig. 5. As the system warms up, the absolute measured position values for (a) method A show an increasing trend over time. The backlash values in (b) are calculated using the relative difference between two corresponding measurements.

To study the impact that thermal expansion has on the backlash measurement procedures, two short experiments were conducted: one for system warm-up and one for system cool-down. For the warm-up test, method A backlash data were collected for 2 min, and the ball screw was then run at high speed and acceleration for 1 min to warm the system. This was repeated for 2 h until the system reached thermal equilibrium. Fig. 5(a) shows the absolute position values measured during the test, and Fig. 5(b) shows the backlash values calculated from these measurements. The absolute position changes by up to $20 \mu\text{m}$. In contrast, the calculated backlash, which is a relative calculation based on two consecutive paired measurements, is less affected by thermal expansion. Over the course of the warm-up period, the backlash value changes by about $0.07 \mu\text{m}$, and after a brief downward trend, the backlash values reach a relatively steady state.

Similarly, a cool-down test is conducted, and method A backlash measurements are taken continuously for 3 h while the system cools down. Over the duration of this experiment, the absolute positions measured by the capacitive sensor again drift by approximately $20 \mu\text{m}$ while the measured backlash values change by a smaller value (around $0.1 \mu\text{m}$). Note that the measured position gap between paired 0^- and 0^+ measurements that is evident in the detailed view inset of Fig. 5(a) is dominated in the full view plot by the thermal trend. These two experiments indicate that the developed backlash measurement methods are resilient to large absolute position changes caused by thermal expansion in the system. Depending on the application industry, the thermal-induced position variation will be larger than the level of backlash that constitutes a system failure, but the calculated backlash values will be within a much smaller range.

For each condition of the RTF experiment, data are collected for all four combinations of two thermal states [cold or transient (i.e., cooling down)] and both the methods (A and B). For each combination, 15–20 backlash measurements are averaged to produce an estimated mean and standard deviation for the backlash at that degradation state.

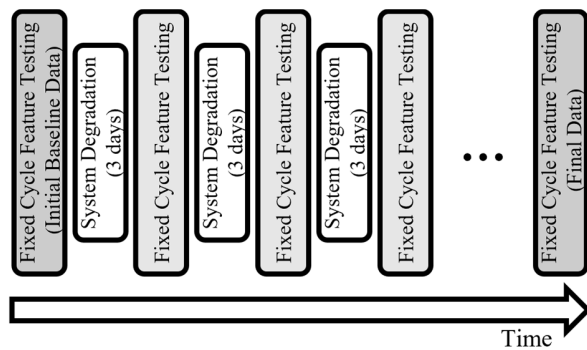


Fig. 6. RTF experiment alternates between a degradation mode comprised of realistic operation profiles and a data acquisition mode to capture the current degradation state.

D. Fixed Cycle Feature Test and RTF Experiment

To observe the development of backlash, a new linear positioning system was operated to degrade the system to the point of failure. During this RTF experiment, the system was operated in two different modes, as shown in Fig. 6. One mode consisted of realistic operation profiles meant to accelerate the degradation of the system, and the other entailed specific data collection strategies for monitoring backlash trends. No lubrication was applied throughout the duration of the experiment to further accelerate the failure.

For the degradation mode, the linear axis was continuously run back and forth with a centered 220-mm-long stroke between 110 and 330 mm (relative to the zero position) with a maximum acceleration magnitude of 9.807 m/s^2 and a nominal maximum speed of 400 mm/s. For each movement, one of the five preset “jitter” patterns was incorporated, in sequence, into the motion as well. For brief and varied lengths of time, while the system was in motion at 400 mm/s, the set speed dropped to between 25% and 75% of the nominal speed before returning to the initial speed. This irregular movement represents the standard operation of a linear axis in industry.

Every three days, the degradation mode is paused, and several sets of data are collected to capture the new degradation state of the system. Vibration and IMU data are collected following the motion profiles described in [25]. This ancillary data can be used to generate indirectly measured backlash trends or estimates. Methods A and B capacitive sensor backlash data are also collected during this pause in degradation. After the system cools fully while paused, the home position is reset, and the degradation pattern resumes.

The RTF experiment sequence covers the complete thermal cycle of the system. For backlash data measurement, the thermal load on the system is minimal, so the system will trend toward (or maintain) a cool state. For other motion profiles, the thermal load on the system increases, and the system trends toward (or maintains) a warm state. The thermal cycle is repeated multiple times throughout the RTF experiment.

The structure of the RTF experiment is intended to mimic practical, real-world applications of backlash measurement for a ball screw system in a production environment where operation is nearly constant. The system degradation pattern represents normal operation requirements for the ball screw mechanism. During any scheduled pause in production,

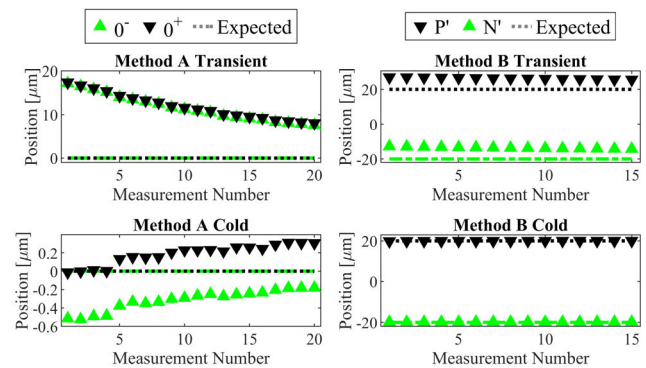


Fig. 7. Individual capacitive sensor position measurements for all measurement types at around 1070 operation hours.

backlash measurements can be acquired to monitor the health of the system in situ and at the submicrometer level with minimal disruption.

While methods A and B procedures can theoretically be used with different sensors or tools, other traditional methods, such as dial indicators, do not allow for the same level of precision in measurements and are therefore not as useful for detecting incipient backlash in high-precision operations. In addition, dial indicators typically have a larger footprint than capacitive sensors and may not be able to remain in place during regular operation, which means additional steps for adding and removing the measurement tool from the system must be taken to collect backlash data. This longer process is not as suitable in real-world scenarios. While an optical grating can offer the same precision as a capacitive sensor and is useful for laboratory-based applications, it is a more expensive, more complex system. The additional cost is not practical for a production environment where many assets may need to be monitored simultaneously. Overall, the capacitive sensor provides a good balance of cost, precision, and ease of use, and experimental data can confirm the utility of backlash measurements using the developed methods.

III. RESULTS AND DISCUSSION

Sample results from around 1070 operation hours are shown in Figs. 7 and 8. Fig. 7 shows the paired position measurement values for all four measurement types. As seen in testing, the transient (cool-down) values for method A show large deviations from $0 \mu\text{m}$ due to thermal effects. As the system cools, the values trend back toward the true home position. Method B transient values also trend downward toward the expected measurement positions at -20 and $20 \mu\text{m}$, but this trend is less significant than the one seen for method A.

The more extreme variation seen in method A transient data is because the most significant cooling happens in the early stages of method A (around the first 10 min). The second half of method A data and method B measurements that follow all experience continually decreasing cooling effects. Methods A and B cold state data show similar, but less distinct, opposite trends. Although the backlash patterns do not warm the system on the same scale as the high-speed patterns, they do produce a slight warming effect on the positions measured by the capacitive sensor. Over the course of method A cold measurements, the thermal expansion causes

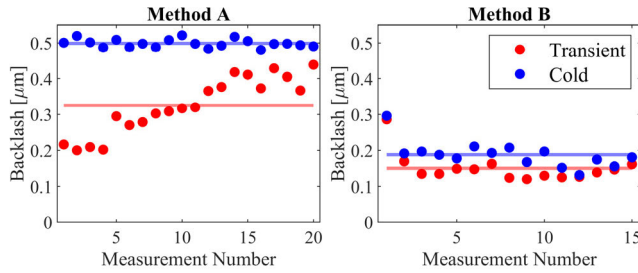


Fig. 8. Calculated backlash measurements for all measurement types at around 1070 operation hours.

TABLE I

STANDARD DEVIATION (IN MICROMETERS) OF POSITIONS AND BACKLASH AROUND 1070 OPERATION HOURS

Method A (All 20 Measurements)			
	0^+	0^-	Backlash
Transient	2.953	3.028	0.079
Cold	0.109	0.111	0.012
Method B (Last 14 Measurements)			
	P^+	N^+	Backlash
Transient	0.421	0.425	0.016
Cold	0.032	0.020	0.022

the absolute home position to drift by approximately $0.3 \mu\text{m}$. This position shift is maintained for method B measurements.

As expected, the effects of position drift due to thermal expansion are not as pronounced for the relative backlash calculations (Fig. 8) as they are for the absolute position measurements. For position shifts of approximately $15 \mu\text{m}$ for method A transient, the calculated backlash values vary from the corresponding cold values by an average of about $0.18 \mu\text{m}$. In addition, as the system cools, the calculated transient values approach the cold state value. In both the method A and method B cases, the cold backlash values are larger than the corresponding transient backlash values, which again follows the observations made in thermal testing.

The effects of thermal expansion are also evident in the standard deviations for each set of measurements. For individual positions, the transient measurements have higher standard deviation values than the corresponding cold measurements, as shown in Table I. These absolute positions show significant deviations that are on the order of the expected incipient backlash measurements; however, since a major source of deviation is thermal expansion rather than random error, the paired $0^+/0^-$ and P^+/N^+ measurements are highly correlated. The developed methods exploit this correlation so that the standard deviation of the relative backlash values for each measurement is, in most cases, an order of magnitude less than the standard deviation for the absolute position measurements.

For method B in both the cold and transient states, the first calculated backlash value appears to be an outlier as it is notably larger than the remaining 14 backlash values in the set. Calculations in Table I and results in Fig. 9 therefore consider only the final 14 measurement sets with the initial outlier value excluded. Furthermore, a very slight downward trend is observed across all 15 backlash values. Both these characteristics are likely tied to the large randomizing reset step that is taken prior to the measurements. The first backlash value, which occurs immediately after the reset step, is the largest. After this, successive measurements incorporate very

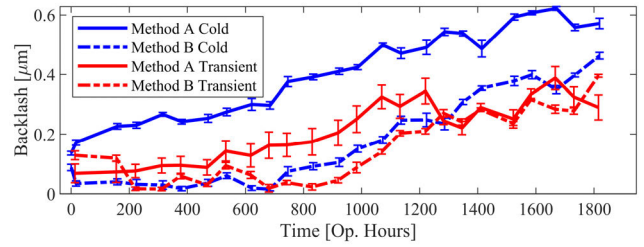


Fig. 9. Backlash measurement results obtained during the RTF experiment using methods A and B. Each measurement method is applied to the system in a cold state and in a transient state (cooling down from a warm state) to study the effects of thermal expansion. The length of each error bar is 1 standard deviation (centered about the mean value) of all measurements taken for each degradation and thermal condition.

small motions ($40 \mu\text{m}$ of movement between -20 and $20 \mu\text{m}$), so the system may get stuck in a local equilibrium that minimizes the true extent of backlash in the system. This can also explain why, on average, method B measurements are lower than method A measurements: method A movements cover $550 \mu\text{m}$ and incorporate more frequent randomizing reset steps.

The average backlash values measured for each method and thermal condition at progressive degradation levels are shown in Fig. 9. The trends for method B and transient method A are all similar. During the initial stages of degradation, the backlash values remain low (less than $0.1 \mu\text{m}$) and fairly constant. This aligns with expectations. In the beginning stages of operational life, the ball screw system is still preloaded to maintain rigidity and precise motion control. While preload exists, the backlash value should be very close to zero. Once preload loss starts, the backlash value will slowly increase as the system degrades.

Method A cold data do not match this trend as clearly, and the backlash values start to increase immediately without an initial period of preload loss. This is possibly due to the additional steps taken to complete the method A measurement procedure, as discussed previously. As error accumulates at each step, the measured backlash value diverges from the true backlash present in the system. This effect is less notable for the transient method A data because the transient state of the system typically shows smaller backlash values overall. Despite the deviation in trend from expectations, method A cold data still pick up a gradually increasing backlash value that can be a relative indicator of degradation development.

As seen previously, the standard deviation of backlash for method A transient ($0.066 \mu\text{m}$ on average) is larger than the standard deviations for the other three methods (0.019 – $0.024 \mu\text{m}$ on average). While methods A and B backlash procedures are able to reduce the extreme effects of thermal deviations, the experimental results confirm that thermal effects do play a role in backlash measurement and need to be carefully considered for incipient backlash detection.

Ultimately, after around 1800 operation hours, the backlash of the system is about $0.5 \mu\text{m}$, depending on which backlash trend is considered. Although the experiment would ideally continue until backlash has developed to a greater extent (at least $10 \mu\text{m}$), this system experienced an unexpected and sudden early failure due to test bed contamination, and the

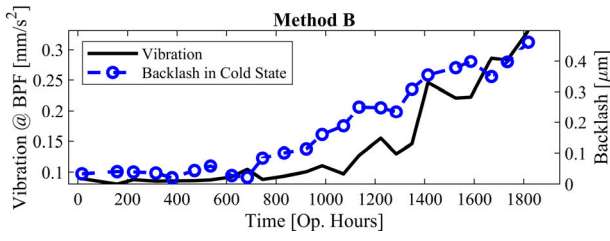


Fig. 10. Method B cold state backlash measurement compared with the BPF feature.

backlash values immediately following those shown in Fig. 9 jump to between 40 and 50 μm . Future RTF experiments will follow the more gradual degradation trend of backlash development, since the cause for the contamination has been eliminated.

Both the proposed backlash methods are theoretically expected to produce an unbiased estimate of the backlash measurement ($E[M_A] = E[M_B] = b$ from (1) and (2)); however, based on the experimental results, the trends produced by method B measurements seem to match expectations more consistently than method A. Method A incorporates five motions (start, reset, 0^- , reset, and 0^+) during which errors can accumulate, while method B incorporates only three motions (reset, P' , and N'). Method A trends do provide a useful general indicator of system health, but given the results of the RTF experiment, the authors recommend that method B measurement procedures are used for monitoring incipient backlash degradation.

Finally, direct backlash measurement from the method B cold system is compared with indirect methods. First, the component of vibration at the BPF of the ball screw is extracted from the vibration data at each stage of degradation. In Fig. 10, the vibration trend and measured backlash trend show similar characteristics as backlash develops in the system. This confirms that indirect measurement methods can be used to predict the relative development of ball screw degradation, but the vibration trend does not quantify the exact level of backlash in the system. Second, a correlation-based method to estimate the backlash via the perceived ball screw pitch [25] yields the presence of incipient backlash ($\leq 2 \mu\text{m}$) until the backlash value immediately following those shown in Fig. 9, which aligns with the results from method B. Therefore, vibration-based and other indirect methods can be used for incipient fault detection when the system is operating under a steady state.

IV. CONCLUSION AND FUTURE WORK

This article explores two different methods of measuring backlash using a capacitive sensor. The measured values are explored for the system in a cold state and in a transient state. Although the measurement procedure can overcome large changes in position due to thermal effects, the backlash values measured on a warmed system during cool-down (a transient state) are less than those measured on a cold system. Therefore, the thermal condition should be carefully considered during backlash measurement, and comparative measurements should be taken for systems of the same relative thermal state.

Based on the results of the RTF experiment, method B measurements most consistently match the expected degradation

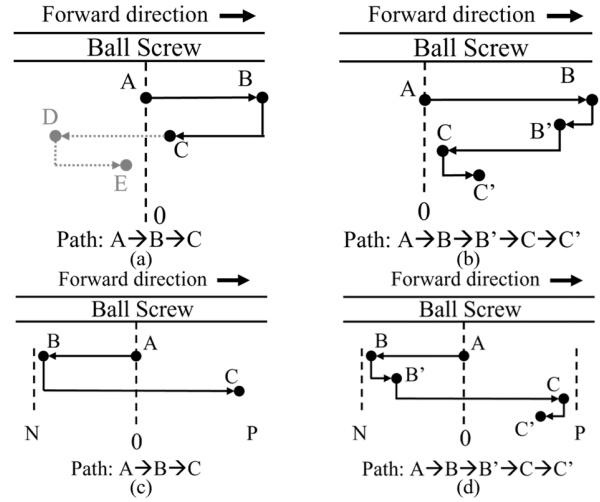


Fig. 11. Backlash measurement models. (a) Model A1: three-point model, (b) model A2: three-point model with bounce error, (c) model B1: path error model, and (d) model B2: path error model with bounce error.

trends. For future experiments, the accuracy of the magnitude of backlash for method B could be improved by increasing the step size and/or incorporating additional randomizing steps. The results also suggest that the errors accumulated during method A measurements may skew the ultimate backlash calculations. While method A already incorporates larger step sizes, and the extracted backlash trend is still useful as a general reference, the systematic errors present in the method A procedure should be further studied to improve the results. Finally, future experiments can explore other potential influences on capacitive sensor measurement outputs, such as ambient temperature and sensor position, to further assess the capabilities of the developed sensor system and backlash measurement method.

Overall, the presented methods can successfully detect the development of initial backlash in ball screws of linear positioning systems. The test procedures consider thermal effects and produce backlash measurements with submicrometer precision. Future testing and modification of the methods based on insights gained from this investigation can confirm the utility of a capacitive sensor-based backlash measurement system for monitoring critical assets in industrial applications.

APPENDIX

Prior Assumptions: The initial position has a random clearance $\Delta \approx U[0, b]$ between the roller and left-side groove; b denotes backlash; the commanded length of motion is d .

Derivation of model A1 (Three-point model without bounce error); see Fig. 11(a):

$$\begin{aligned} A &= 0 \\ B &= d - \Delta, \quad \Delta \approx U[0, b] \\ C &= B - (d - b) = b - \Delta. \end{aligned} \quad (3)$$

Backlash measurement M : $M = C - A = b - \Delta$

$$E[M] = b - \frac{b}{2} = \frac{b}{2}, \quad V[M] = \frac{b^2}{12}. \quad (4)$$

$E[M]$ in model A1 indicates forward error accumulation after multiple cycles, which is invalid because the machine

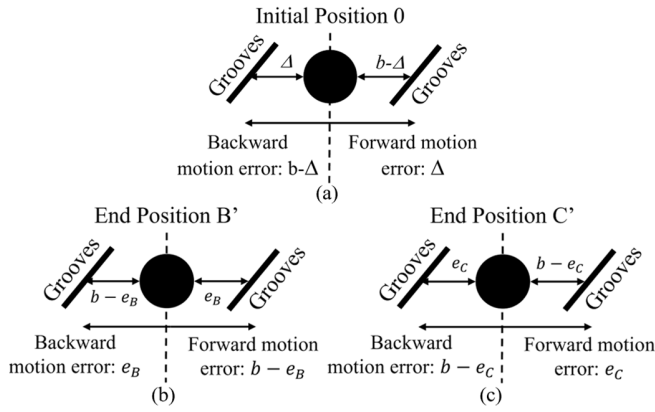


Fig. 12. Illustration of bounce error in model A2. (a) Random initial condition. (b) Random end position of the roller at B' with bounce error e_B . (c) Random end position of the roller at C' with bounce error e_C .

should be repeatable. To fix this, we add a negative path, as indicated by the dotted line from C to E in Fig. 11(a). The Δ in the measurement will be canceled by the negative path. The basic idea for model A3, referred to as the five-point model, is based on the inclusion of a negative path. Another solution, explored in model A2, is adding a bounce error.

Derivation of model A2 (Three-point model with bounce error): model A2 is established by introducing a bounce error to model A1, where $e_B = B - B'$, $e_B \approx U[0, b]$, $e_C = C' - C$, $e_C \approx U[0, b]$, and b denotes the backlash; see Fig. 12

$$\begin{aligned} A &= 0 \\ B &= d - \Delta \\ B' &= B - e_B = d - \Delta - e_B, \quad e_B \approx U[0, b] \\ C &= B' - [d - (b - e_B)] = b - \Delta - 2e_B \\ C' &= C + e_C = b - \Delta - 2e_B + e_C, \quad e_C \approx U[0, b] \\ M &= C' - A = b - \Delta - 2e_B + e_C \end{aligned} \quad (5)$$

$$E[M] = 0, \quad V[M] = 4 \times \frac{b^2}{12} = \frac{b^2}{3}. \quad (6)$$

Different from model A1, $E[M]$ in (7) indicates no error accumulation after repeating the operation multiple times. It is important to include bounce error in the model.

Derivation of model A3 (Five-point model): model A3 is established by mirroring the forward path of model A1 in the negative direction. Following the same derivation procedure as in model A1, the backlash model A3 is shown in (8).

$$\begin{aligned} M &= C - E = b \\ E[M] &= b, \quad V[M] = 0. \end{aligned} \quad (7)$$

Despite the imperfection of the hypothesis in model A1, the measurement $M = C - E$ in model A3 indicates that this method can be used to measure the backlash.

Derivation of model B1 (Path error model without bounce error): Instead of a point estimate, model B1 considers the path error $(P - N) - (P' - N')$ where $P - N$ denotes the ideal length of the path and $P' - N'$ denotes the actual length that is measured by the capacitive sensor

$$\begin{aligned} A &= 0 \\ N' &= B = -d + b - \Delta \end{aligned} \quad (8)$$

$$\begin{aligned} P' &= C = d - \Delta, \quad \Delta \approx U[0, b] \\ M &= (P - N) - (P' - N') = b. \end{aligned} \quad (9)$$

Model B1 provides an unbiased estimate of the backlash.

Derivation of model B2 (Path error model with bounce error): model B2 introduces bounce error to model B1

$$\begin{aligned} A &= 0 \\ B &= -d + b - \Delta \end{aligned} \quad (10)$$

$$N' = B' = -d + b - \Delta + e_B, \quad e_B \approx U[0, b]$$

$$C = d - \Delta - 2e_B$$

$$P' = C' = d - \Delta + 2e_B - e_C, \quad e_C \approx U[0, b]$$

$$M = (P - N) - (P' - N') = b - e_B + e_C$$

$$E[M] = b - \frac{b}{2} + \frac{b}{2} = b, \quad V[M] = \frac{b^2}{6}. \quad (11)$$

NIST DISCLAIMER

Certain commercial equipment, instruments, or materials are identified in this article to specify the experimental procedure adequately. Such identification is not intended to imply recommendation or endorsement by the National Institute of Standards and Technology, nor is it intended to imply that the materials or equipment identified are necessarily the best available for the purpose. This material is declared a work of the U.S. Government and is not subject to copyright protection in the United States. Approved for public release; distribution is unlimited.

REFERENCES

- Y. Altintas, A. Verl, C. Brecher, L. Uriarte, and G. Pritschow, "Machine tool feed drives," *CIRP Ann.*, vol. 60, no. 2, pp. 779–796, 2011, doi: [10.1016/j.cirp.2011.05.010](https://doi.org/10.1016/j.cirp.2011.05.010).
- K. Miyaguchi and S. Arai, "State of the art ball screw trends for machine tool applications," *J. SME-Japan*, vol. 2, pp. 13–18, Jul. 2013. [Online]. Available: <https://www.sme-japan.org/journal2-nsk.pdf>
- H. Li, J. Yang, and Y. Li, "Axial contact stiffness analysis of the ball screw for aerospace electromechanical servo system," in *Proc. 2nd World Conf. Mech. Eng. Intell. Manuf. (WCMEIM)*, Nov. 2019, pp. 45–49, doi: [10.1109/WCMEIM48965.2019.00016](https://doi.org/10.1109/WCMEIM48965.2019.00016).
- C.-C. Wei, W.-L. Liou, and R.-S. Lai, "Wear analysis of the offset type preloaded ball-screw operating at high speed," *Wear*, vols. 292–293, pp. 111–123, Jul. 2012, doi: [10.1016/j.wear.2012.05.024](https://doi.org/10.1016/j.wear.2012.05.024).
- C.-G. Zhou, H.-X. Zhou, and H.-T. Feng, "Experimental analysis of the wear coefficient of double-nut ball screws," *Wear*, vols. 446–447, Apr. 2020, Art. no. 203201, doi: [10.1016/j.wear.2020.203201](https://doi.org/10.1016/j.wear.2020.203201).
- H. Schwenke, W. Knapp, H. Haitjema, A. Weckenmann, R. Schmitt, and F. Delbressine, "Geometric error measurement and compensation of machines—An update," *CIRP Ann.*, vol. 57, no. 2, pp. 660–675, 2008, doi: [10.1016/j.cirp.2008.09.008](https://doi.org/10.1016/j.cirp.2008.09.008).
- T. Mcnier and J. G. Johnson. *Specifying, Selecting and Applying Linear Ball Screw Drives*. Accessed: Mar. 23, 2024. [Online]. Available: http://www.thomsonlinear.com/downloads/articles/specifying_selecting_applying_linear_ball_screw_drives_tnen.pdf
- H. Yang et al., "Remaining useful life prediction of ball screw using precision indicator," *IEEE Trans. Instrum. Meas.*, vol. 70, pp. 1–9, 2021, doi: [10.1109/TIM.2021.3087803](https://doi.org/10.1109/TIM.2021.3087803).
- P. Tsai, C. Cheng, and Y. Hwang, "Ball screw preload loss detection using ball pass frequency," *Mech. Syst. Signal Process.*, vol. 48, nos. 1–2, pp. 77–91, 2014, doi: [10.1016/j.ymsp.2014.02.017](https://doi.org/10.1016/j.ymsp.2014.02.017).
- T. L. Nguyen, S.-K. Ro, C. K. Song, and J.-K. Park, "Study on preload monitoring of ball screw feed drive system using natural frequency detection," *J. Korean Soc. Precis. Eng.*, vol. 35, no. 2, pp. 135–143, Feb. 2018, doi: [10.7736/kspe.2018.35.2.135](https://doi.org/10.7736/kspe.2018.35.2.135).
- T. L. Nguyen, S.-K. Ro, and J.-K. Park, "Study of ball screw system preload monitoring during operation based on the motor current and screw-nut vibration," *Mech. Syst. Signal Process.*, vol. 131, pp. 18–32, Sep. 2019, doi: [10.1016/j.ymsp.2019.05.036](https://doi.org/10.1016/j.ymsp.2019.05.036).

- [12] P. Li et al., "Prognosability study of ball screw degradation using systematic methodology," *Mech. Syst. Signal Process.*, vol. 109, pp. 45–57, Sep. 2018, doi: [10.1016/j.ymssp.2018.02.046](https://doi.org/10.1016/j.ymssp.2018.02.046).
- [13] H.-X. Zhou, C.-G. Zhou, X.-Y. Wang, H.-T. Feng, and J.-L. Xie, "Degradation reliability modeling for two-stage degradation ball screws," *Precis. Eng.*, vol. 73, pp. 347–362, Jan. 2022, doi: [10.1016/j.precisioneng.2021.09.018](https://doi.org/10.1016/j.precisioneng.2021.09.018).
- [14] A. C. Bertolino, M. Sorli, G. Jacazio, and S. Mauro, "Lumped parameters modelling of the EMAs' ball screw drive with special consideration to ball/grooves interactions to support model-based health monitoring," *Mechanism Mach. Theory*, vol. 137, pp. 188–210, Jul. 2019.
- [15] Z. Geng, Z. Tong, and X. Jiang, "Review of geometric error measurement and compensation techniques of ultra-precision machine tools," *Light. Adv. Manuf.*, vol. 2, no. 2, p. 211, 2021, doi: [10.37188/lam.2021.014](https://doi.org/10.37188/lam.2021.014).
- [16] J. Liu, C. Ma, and S. Wang, "Precision loss modeling method of ball screw pair," *Mech. Syst. Signal Process.*, vol. 135, Jan. 2020, Art. no. 106397, doi: [10.1016/j.ymssp.2019.106397](https://doi.org/10.1016/j.ymssp.2019.106397).
- [17] Q. Cheng, B. Qi, Z. Liu, C. Zhang, and D. Xue, "An accuracy degradation analysis of ball screw mechanism considering time-varying motion and loading working conditions," *Mechanism Mach. Theory*, vol. 134, pp. 1–23, Apr. 2019, doi: [10.1016/j.mechmachtheory.2018.12.024](https://doi.org/10.1016/j.mechmachtheory.2018.12.024).
- [18] H. Haitjema, "Calibration of displacement laser interferometer systems for industrial metrology," *Sensors*, vol. 19, no. 19, p. 4100, Sep. 2019, doi: [10.3390/s19194100](https://doi.org/10.3390/s19194100).
- [19] R. Ramesh, M. A. Mannan, and A. N. Poo, "Error compensation in machine tools—A review," *Int. J. Mach. Tools Manuf.*, vol. 40, no. 9, pp. 1257–1284, Jul. 2000, doi: [10.1016/s0890-6955\(00\)00010-9](https://doi.org/10.1016/s0890-6955(00)00010-9).
- [20] Z. Li, K. Fan, J. Yang, and Y. Zhang, "Time-varying positioning error modeling and compensation for ball screw systems based on simulation and experimental analysis," *Int. J. Adv. Manuf. Technol.*, vol. 73, nos. 5–8, pp. 773–782, Jul. 2014, doi: [10.1007/s00170-014-5865-9](https://doi.org/10.1007/s00170-014-5865-9).
- [21] S. Yang, J. Yuan, and J. Ni, "The improvement of thermal error modeling and compensation on machine tools by CMAC neural network," *Int. J. Mach. Tools Manuf.*, vol. 36, no. 4, pp. 527–537, Apr. 1996, doi: [10.1016/0890-6955\(95\)00040-2](https://doi.org/10.1016/0890-6955(95)00040-2).
- [22] S. Böhl, S. Weikert, and K. Wegener, "Enhancing signal quality of capacitive displacement measurements in machine tool environments," *J. Manuf. Mater. Process.*, vol. 3, no. 3, p. 76, Aug. 2019, doi: [10.3390/jmmp3030076](https://doi.org/10.3390/jmmp3030076).
- [23] J. Józwiak, "Dynamic measurement of spindle errors of CNC machine tools by capacitive sensors during aircraft parts machining," in *Proc. 5th IEEE Int. Workshop Metrology Aersp. (MetroAeroSpace)*, Jun. 2018, pp. 398–402, doi: [10.1109/METROAEROSPACE.2018.8453508](https://doi.org/10.1109/METROAEROSPACE.2018.8453508).
- [24] C. Li, M. Xu, W. Song, and H. Zhang, "A review of static and dynamic analysis of ball screw feed drives, recirculating linear guideway, and ball screw," *Int. J. Mach. Tools Manuf.*, vol. 188, May 2023, Art. no. 104021, doi: [10.1016/j.ijmactools.2023.104021](https://doi.org/10.1016/j.ijmactools.2023.104021).
- [25] V. Pandhare, M. Miller, G. W. Vogl, and J. Lee, "Ball screw health monitoring with inertial sensors," *IEEE Trans. Ind. Informat.*, vol. 19, no. 6, pp. 7323–7334, Jun. 2023, doi: [10.1109/TII.2022.3210999](https://doi.org/10.1109/TII.2022.3210999).
- [26] G. W. Vogl, M. A. Donmez, and A. Archenti, "Diagnostics for geometric performance of machine tool linear axes," *CIRP Ann.*, vol. 65, no. 1, pp. 377–380, 2016, doi: [10.1016/j.cirp.2016.04.117](https://doi.org/10.1016/j.cirp.2016.04.117).
- [27] J.-W. Shen, H.-T. Feng, C.-G. Zhou, Z.-T. Chen, and Y. Ou, "A new two-stage degradation model for the preload of ball screws considering geometric errors," *Wear*, vols. 500–501, Jul. 2022, Art. no. 204352, doi: [10.1016/j.wear.2022.204352](https://doi.org/10.1016/j.wear.2022.204352).



Marcella Miller received the B.S. and M.Eng. degrees in mechanical engineering from the University of Cincinnati, Cincinnati, OH, USA, in 2019, where she is currently pursuing the Ph.D. degree in mechanical engineering with the Department of Mechanical and Materials Engineering.

Her research interests include prognostics and health management, machine learning, and probabilistic methods.



Xu Han received the B.S. degree in mechanical engineering from the University of Cincinnati, Cincinnati, OH, USA, and Chongqing University, Chongqing, China, in 2020, and the M.S. degree in mechanical engineering from the University of Cincinnati, in 2024, where he is currently pursuing the Ph.D. degree in mechanical engineering with the Department of Mechanical and Materials Engineering.

His research interests include prognostics and health management, machine learning, and intelligent metrology.



Gregory William Vogl received the bachelor's degree in engineering science and mechanics and the master's and the Ph.D. degree in engineering mechanics from Virginia Polytechnic Institute and State University of Blacksburg, Blacksburg, VA, USA, in 2000, 2003, and 2006, respectively.

After a National Research Council Post-Doctoral fellowship at the National Institute of Standards and Technology (NIST), he joined the Production Systems Group at NIST and worked on machine tool standards and vibration metrology. Currently,

he leads the Augmented Intelligence for Manufacturing Systems (AIMS) project, which seeks to develop augmented intelligent solutions for manufacturing systems.

Dr. Vogl was elected as an Associate Member of the International Academy for Production Engineering (CIRP), in 2023.



Anita Penkova received the B.S. degree in engineering from the Department of design of apparatus for industry applications and the M.S. degree in chemical engineering from the University of Chemical Technology and Metallurgy, Sofia, Bulgaria, in 1991 and 1992, respectively, and the Ph.D. degree in physical chemistry from the Bulgarian Academy of Sciences, Sofia, in 2007.

She joined the University of Zurich, Switzerland, Zurich as a Post-Doctoral Associate in 2007 and the University of Southern California (USC), Los Angeles, CA, USA, in 2008 to work on the ocular biotransport projects and teach engineering thermodynamics, holding the position of an Assistant Professor, Research, at the Aerospace and Mechanical Engineering Department. Currently, she is the CEO of her start-up company on big data in biotransport and healthcare. Her research interests include ocular fluid dynamics, ML, and transport phenomena associated with drug delivery.

Her research interests include ocular fluid dynamics, ML, and transport phenomena associated with drug delivery.



Xiaodong Jia received the B.S. degree in engineering thermodynamics from Central South University, Changsha, China, in 2008, the M.S. degree in mechanical engineering from Shanghai Jiao Tong University, Shanghai, China, in 2014, and the Ph.D. degree in mechanical engineering from the University of Cincinnati, Cincinnati, OH, USA, in 2018.

He is currently an Assistant Professor with the Department of Mechanical and Materials Engineering, University of Cincinnati. His research interests include prognostics and health management, data mining, and ML.